Received: 10 April 2020 | Revised: 5 October 2020 | Accepted: 9 October 2020

DOI: 10.1002/hbm.25255

WILEY

RESEARCH ARTICLE

Dissimilarity of functional connectivity uncovers the influence of participant's motion in functional magnetic resonance imaging studies

Lili Yang[1] | Bo Wu[2] | Linyu Fan[1] | Shishi Huang[3] | Andrew D. Vigotsky[4] | Marwan N. Baliki[5,6] | Zhihan Yan[1] | A. Vania Apkarian[7,8] | Lejian Huang[7,8]

[1]Department of Radiology, The Second Affiliated Hospital and Yuying Children's Hospital of Wenzhou Medical University, Wenzhou, Zhejiang, China

[2]Department of Information, The Second Affiliated Hospital and Yuying Children's Hospital of Wenzhou Medical University, Wenzhou, Zhejiang, China

[3]Department of Neurology, The Second Affiliated Hospital and Yuying Children's Hospital of Wenzhou Medical University, Wenzhou, Zhejiang, China

[4]Departments of Biomedical Engineering and Statistics, Northwestern University, Evanston, Illinois

[5]Shirley Ryan AbilityLab, Chicago, Illinois

[6]Department of Physical Management and Rehabilitation, Northwestern University Feinberg School of Medicine, Chicago, Illinois

[7]Department of Physiology, Northwestern University Feinberg School of Medicine, Chicago, Illinois

[8]Center for Translational Pain Research, Northwestern University Feinberg School of Medicine, Chicago, Illinois

Correspondence
Lejian Huang, A. Vania Apkarian, and Zhihan Yan, Department of Physiology, Northwestern University, Chicago, IL 60611.
Email: lejian-huang@northwestern.edu (L. H.), a-apkarian@northwestern.edu (A. V. A.), yanzhihanwz@163.com (Z. Y.)

Funding information
National Institutes of Health, Grant/Award Number: 1P50DA044121-01A1; National Science Foundation, Grant/Award Number: DGE-1324585

Abstract

Head motion is a major confounding factor impairing the quality of functional magnetic resonance imaging (fMRI) data. In particular, head motion can reduce analytical efficiency, and its effects are still present even after preprocessing. To examine the validity of motion removal and to evaluate the remaining effects of motion on the quality of the preprocessed fMRI data, a new metric of group quality control (QC), dissimilarity of functional connectivity, is introduced. Here, we investigate the association between head motion, represented by mean framewise displacement, and dissimilarity of functional connectivity by applying four preprocessing methods in two independent resting-state fMRI datasets: one consisting of healthy participants (N = 167) scanned in a 3T GE-Discovery 750 with longer TR (2.5 s), and the other of chronic back pain patients (N = 143) in a 3T Siemens Magnetom Prisma scanner with shorter TR (0.555 s). We found that dissimilarity of functional connectivity uncovers the influence of participant's motion, and this relationship is independent of population, scanner, and preprocessing method. The association between motion and dissimilarity of functional connectivity, and how the removal of high-motion participants affects this association, is a new strategy for group-level QC following preprocessing.

KEYWORDS

dissimilarity, fMRI, functional connectivity, group quality of control, motion

1 | INTRODUCTION

Head motion always exists during magnetic resonance imaging (MRI) acquisitions, particularly when children, elderly, and patients (e.g., with chronic pain or Parkinson's disease) are scanned (Alfaro-Almagro et al., 2018; Igata et al., 2017; Malfliet et al., 2017; Satterthwaite et al., 2012; Yuan et al., 2009). Moreover, head motion is considered one of the major confounding factors impairing the quality of functional MRI (fMRI) data and consequently reducing analytical efficiency (Ciric et al., 2018). Thus, a wide variety of preprocessing methods have been proposed to mitigate motion-related artifacts prior to analysis. These methods include (a) the conventional method (Baliki et al., 2012), which covers motion correction (Jenkinson, Bannister, Brady, & Smith, 2002), slice-time correction (Sladky et al., 2011), low-frequency signal drift (Smith et al., 1999), spatial smoothing (Smith & Brady, 1997), band-pass temporal filtering, and regressions of physiological signals within white matter (WM) and cerebrospinal fluid (CSF), motion-related parameters, and global signal (Murphy, Birn, Handwerker, Jones, & Bandettini, 2009); (b) the scrubbing method, which involves removing volumes that exceed some motion threshold (Power et al., 2014); and two ICA-based methods; (c) Automatic Removal of Motion Artifacts (ICA-AROMA) (Pruim et al., 2015); and (d) FMRIB's ICA-based Xnoiseifier (FIX) (Salimi-Khorshidi et al., 2014). At the participant level, the aforementioned methods could greatly reduce motion-related artifacts based on a series of benchmarks (Parkes, Fulcher, Yucel, & Fornito, 2018); however, it is conceivable that none of the methods are able to remove all artifacts in the presence of head motion to such a level that compares to the ideal no-motion condition. Specifically, even minor motion between volumes during image acquisition will contribute to major intensity shifts in BOLD data (Parkes et al., 2018; Zaitsev, Akin, LeVan, & Knowles, 2017), which will influence the correlations between signals depending on the waveforms of the confounds. Thus, it is imperative to develop group-based quality control (QC) strategies, examine the validity of motion removal, and evaluate the remaining effects of motion on the quality of the preprocessed fMRI data.

One group-based QC strategy is to select the participant-level preprocessing method that minimizes a group-level metric of motion. For example, QC-FC correlation is a commonly used group-level metric in which motion, represented by mean framewise displacement (FD) over all volumes, is correlated with all possible pair-wise functional connectivity (FC) correlations across participants in a group, reflecting the extent to which motion may modulate FC (Power, Schlaggar, & Petersen, 2015). Another strategy, derived from the central limit theorem (Paulauskas & Rachkauskas, 1989), is to remove participant(s) with motion-related features that stand out from the rest in the group. In (Huang et al., 2019), a motion-related feature, similarity of FC (SoFC), was introduced, in which the participants with a mean similarity of less than 2 *SD*s from the average of the healthy control or patient group were excluded from further analyses. However, this participant-level removal of motion effect assumes that the distributions of motion-related features of groups from different populations are approximately equivalent; this assumption is violated by our observation that patients generally have greater motion than healthy participants. As a consequence, it may introduce systematic bias, which may be especially pronounced in group comparisons between patients and controls (Parkes et al., 2018). In this paper, we suggest a new group-level QC metric, which is an extension of QC-FC correlations, to quantify how an individual participant's motion affects the quality of preprocessed fMRI data. Based on this metric, a new group-based QC strategy is proposed, wherein participants in either healthy or patient groups will be removed to maximally reduce the coupling between motion and FC at the group level.

Accordingly, in this paper, first, a new group-based QC metric, SoFC, is introduced in detail. Following this, the relationship between head motion, represented by FD and dissimilarity of FC with four commonly used preprocessing methods, is investigated in two independent resting-state fMRI datasets: one consisting of healthy participants scanned in a GE scanner with longer TR and the other of chronic back pain (CBP) patients in a Siemens scanner with shorter TR. Finally, after exploring the effect of removing participants with the greatest amount of motion in a given group on the SoFC, a new group-based QC strategy is proposed.

2 | METHODS

2.1 | Participants

A total of 310 participants from two independent studies were included. Study 1 (healthy participants) was carried out at Wenzhou Medical University, Zhejiang, China, and included 167 healthy volunteers (83 males, 84 females; age [mean ± *SD*] = 40.9 ± 14.1 years old) who were pain-free for at least 52 weeks prior to recruitment. Study 2 (CBP participants) was carried out at Northwestern University, IL, and consisted of 143 of CBP patients (71 males, 72 females; age = 52.5 ± 13.6 years old) with pain that persisted for at least 12 weeks prior to recruitment. Participants were excluded if they (a) were less than 18 or greater than 85 years old; (b) reported a history of head injury and/or cerebral disease (e.g., stroke or encephalopathy); (c) had diabetes or a psychiatric disease; (d) reported a history of brain neurosurgical procedures and/or epilepsy; (e) were unable to cooperate (e.g., psychogenic or cognitively impaired); (f) reported pregnancy, drug dependence, or drug abuse; (g) were not suitable for MRI scan; or (h) were enrolled in other clinical trial(s) involving investigational drug(s).

The studies were approved by the Institutional Review Board of the Second Affiliated Hospital and Yuying Children's Hospital of Wenzhou Medical University, China and of Northwestern University, and all participants reviewed and signed a written informed consent.

2.2 | MRI scanning parameters

All participants were scanned for structural and resting-state fMRI (rs-fMRI) and were instructed to keep their eyes open and to remain as

still as possible during acquisition. Healthy participants were scanned on a 3 Tesla GE-Discovery 750 whole body scanner equipped with an eight channel-head/neck coil. T1-anatomical brain images were acquired with the following parameters: voxel size = $1 \times 1 \times 1$ mm^3; repetition time/echo time (TR/TE) = 7.7/3.4 ms; flip angle = 12°; in-plane resolution = 256×256; slices per volume = 176; field of view = 256 mm. Rs-fMRI images were acquired on the same day with the following parameters: TR/TE = 2,500/30 ms; flip angle = 90°; voxel size = $3.4375 \times 3.4375 \times 3.5$ mm^3; in-plane resolution = 64×64; number of volumes = 230; number of slices = 42 acquired with interleaved ordering, which covers the whole brain from the cerebellum to the vertex.

CBP participants were scanned on a clinical 3 Tesla Siemens Magnetom Prisma whole body scanner equipped with a 64 channel-head/neck coil. T1-anatomical brain images were acquired using integrated parallel imaging techniques (GRAPPA) with the following parameters: voxel size = $1 \times 1 \times 1$ mm^3; TR/TE = 2.3 s/2.40 ms; flip angle = 9°; in-plane resolution = 256×256; slices per volume = 176; field of view = 256 mm. Rs-fMRI images were acquired on the same day with the following parameters: TR/TE = 555/22 ms; flip angle = 47°; voxel size = $2 \times 2 \times 2$ mm^3; in-plane resolution = 96×104; number of volumes = 1,110; multiband accelerator = 8; number of slices = 64 acquired with interleaved ordering, which covers the whole brain from the cerebellum to the vertex.

2.3 | Measurement of head motion

FD is a measure of head motion of one volume from one time point to the next, and is calculated as the sum of absolute value of the three translational displacements (x, y, and z) and the three rotational displacements (pitch, yaw, and roll, in radians); the latter were multiplied by 50 to convert to arc length displacements in the same units as translational displacements (i.e., $FD = |x| + |y| + |z| + 50(\alpha + \beta + \gamma)$) (Power et al., 2014). Mean FD (mFD), calculated as the average FD across all time points except the first one, represents the extent of head motion over the duration of the scan.

2.4 | Calculating SoFC within a group

FC represents symmetrical statistical associations among brain regions of interest (ROIs) and is defined as the temporal correlations between BOLD signals of different ROIs. SoFC represents the resemblance of FC of one participant to all other participants within a group. Figure 1 depicts the calculation of SoFC within a group comprising N participants. As shown in Figure 1a, for each participant, 264 ROIs defined in (Power et al., 2011) were used to construct ROI-based pairwise FC. The BOLD signal of each ROI was extracted as the average over voxels within 10 mm diameter spheres centered at peak coordinates.

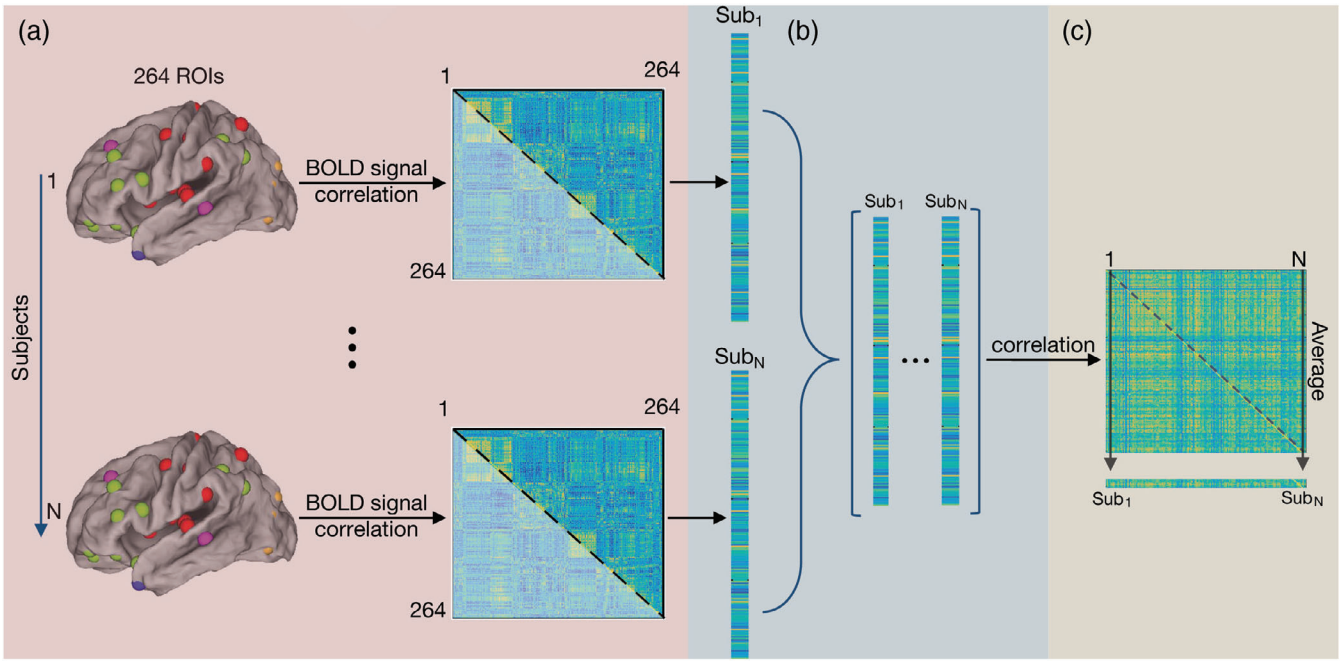

FIGURE 1 Diagram illustrates main steps required to calculate similarity of functional connectivity within a group. (a) For each participant in a group comprising N participants, 264 regions of interest (ROIs) defined in (Power et al., 2011) were used to construct ROI-based functional networks. The BOLD signal of each ROI was extracted as an average over voxels within 10 mm diameter spheres centered at peak coordinates. Following this, a 264×264 correlation matrix was generated using Pearson correlation coefficients between BOLD signals. (b) The upper (or lower) triangular correlation matrix of each participant was transformed into a vector; these vectors were combined to create $(264 \times 263)/2 \times N$ matrix, each column of which represents functional connectivity of each participant across all pairs of the 264 ROIs. (c) Correlation coefficients of functional connectivity of N participants were calculated and a $N \times N$ matrix was generated; the average of each column excluding the diagonal was calculated, representing the similarity of each participant's functional connectivity to the rest of the sample

Following this, a 264 × 264 correlation matrix was generated, consisting of Pearson correlation coefficients between BOLD signals. The upper (or lower) triangular correlation matrix of each participant was then transformed into a vector; these vectors were combined to create a (264 × 263)/2 × *N* matrix, each column of which represents FC of each participant across all pairs of the 264 ROIs (Figure 1b). Finally, correlation coefficients of FC of *N* participants were calculated and an *N* × *N* matrix was generated. After excluding the diagonal, column means were calculated to obtain the similarity of each participant's FC to the rest of the sample (Figure 1).

2.5 | Rs-fMRI data preprocessing

In this study, to explore the relationship between head motion represented by mFD and SoFC for both healthy and CBP participants and to investigate the effect of preprocessing methods on the relationship, four commonly used methods—*conventional* (Baliki et al., 2012), *scrub* (Power et al., 2014), *ICA-AROMA* (Pruim et al., 2015), and *FIX* (Salimi-Khorshidi et al., 2014)—were performed on the same datasets.

As shown in Figure 2, all four preprocessing methods performed the following common steps: First, using the FMRIB Expert Analysis Tool (www.fmrib.ox.ac.uk/fsl), MATLB2016a, and Bash Shell Scripting, we discarded of the first 10-s of images for magnetic field stabilization; motion correction; slice-time correction; intensity normalization; high-pass temporal filtering (0.0075 Hz) for correcting low-frequency signal drift; and a nonlinear spatial smoothing (using SUSAN; FWHM = 6 mm). Second, for the *conventional* approach, after the remaining volumes were filtered with a band-pass temporal filter (using Butterworth; 0.008 Hz < f < 0.1 Hz), regressions were performed using the CSF signal averaged over all voxels of the eroded ventricle region, the averaged WM signal, the averaged global signal of the whole brain, and the six parameters obtained from intra-modal motion correction using MCFLIRT; for *scrub*, motion-volumes were censored by detecting volumes with (a) an FD larger than 0.5 mm, (b) a derivative variance root mean square after Z normalization larger than 2.3, (c) *SD* after Z normalization larger than 2.3, and (d) scrubbing above detected and adjacent symmetric 10-s volumes; for *ICA-AROMA*, after classing and regressing components that represent motion-related artifacts by assessing each component as to whether it exceeded at least one of three criteria: (a) a decision value determined by a linear discriminant analysis that combines brain edge fractions with the maximum correlations with motion-correction parameters, (b) 10% of the CSF fraction, or (c) 35% of the high-frequency content, and regressions were performed using the CSF signal averaged over all voxels of eroded ventricle region, averaged WM signal, averaged global signal of whole brain and the processed image data were filtered with a band-pass temporal filter (using Butterworth; 0.008 Hz < f < 0.1 Hz) in the end; for *FIX*, after automatically classifying and regressing out "bad" components by applying the classifier derived from training data based on their spatial and/or temporal features, regression was performed using the averaged global signal of whole brain, and finally, the processed image data were filtered with a band-pass temporal filter (using Butterworth; 0.008 Hz < f < 0.1 Hz). Standard.Rdata provided by FSL were fed as trained-weight files for *FIX*-preprocessing of healthy participants. For CBP participants, self-trained-weights files were supplied to *FIX*, where components in 10 subjects randomly selected from the data set were hand classified as either noise or signal components. Twenty was set as the thresholding of good versus bad components for both data sets.

All pre-processed rs-fMRI data were registered to MNI_152_2mm template using FNIRT (ref. https://www.fmrib.ox.ac.uk/datasets/

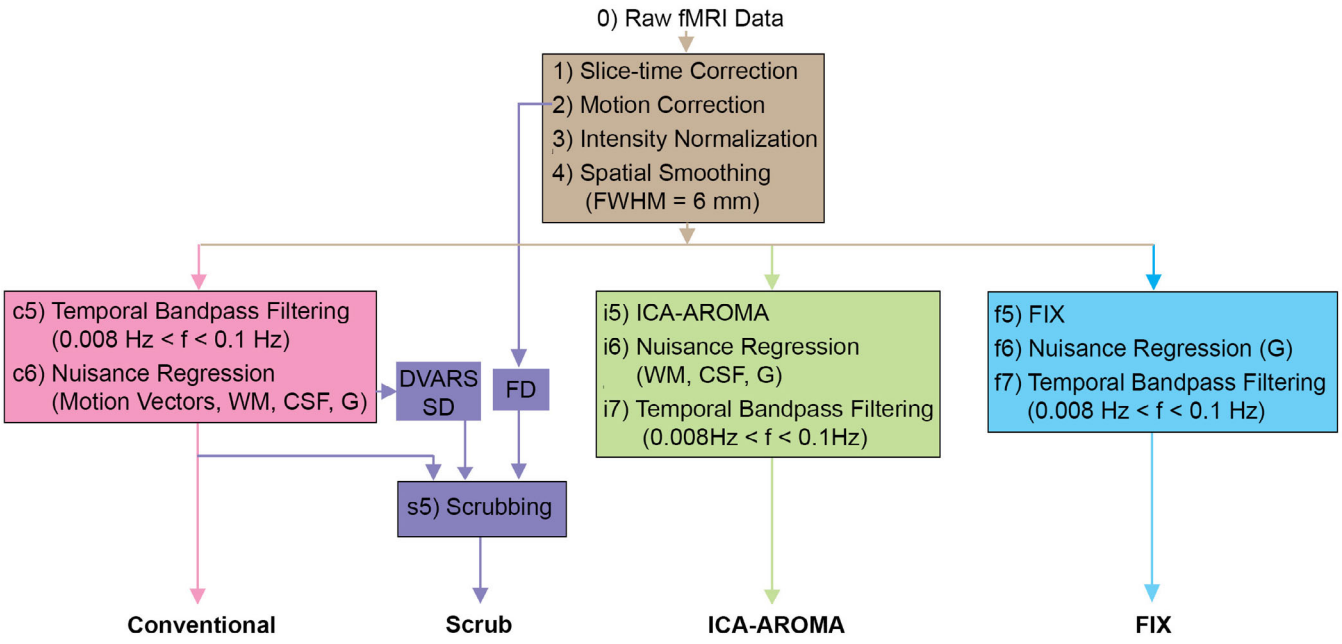

FIGURE 2 Flowchart of four preprocessing methods

techrep/tr07ja2/tr07ja2.pdf) for postprocessing. To investigate the effect of the population template on our findings, all data from China were also registered to CN200 template and reanalyzed (Yang et al., 2020).

2.6 | The effects of the greatest-motion participants on SoFC

In this study, we used two approaches (removal or addition of greatest-motion participants) to investigate the effects of greatest-motion participants on SoFC. The first one was to gradually remove the greatest-motion participants from the study group and estimate the regression slope between mFD and SoFD in the remaining participants. The second one was to gradually add greater-motion participants to a given subgroup consisting of less-motion participants and then recalculate the SoFCs within its subgroup. Considering that SoFC is dependent on the size of a given group when individuals are added nonrandomly (i.e., here, the bigger the size of the group, the lower the SoFC in the group due to increased variance), the identical number of participants in the subgroup is necessary for the second approach. To satisfy this requirement, first, based on the value of mFD, either the entire healthy or CBP group was divided into two subgroups: those with greater motion (top 20%) and those with lesser motion (bottom 80%). One participant at a time, we replaced a random lower-motion participant with the participant with the greatest motion. This was repeated until all of the high-motion (top 20%) participants were added. For example, if there are 80 low-motion and 20 high-motion participants, one of the 80 low-motion participants would be randomly replaced by the participant with the greatest motion; next, one randomly selected participant from the 79 remaining low-motion participants would be replaced by the participant with the second-greatest motion; and so on. The SoFC of each participant in the new "lesser" motion group was recalculated after a participant was replaced. Finally, only participants in the lesser motion subgroup were extracted and used for further analysis (healthy [101 participants] and CBP [85 participants]). By using this strategy, the effect of gradually adding greater-motion participants (0–20%) on the SoFCs of participants with lower motion (60% of lower motion, in that 20% of participants with lower motion would be replaced by greater-motion participants) could be investigated while maintaining identical sample sizes.

2.7 | Statistical analyses

The Pearson product–moment correlation coefficient was used to quantify the strength of the linear relationship between mFD and SoFC. A negative correlation coefficient with $p < .001$ represents a statistically significant association between motion and dissimilarity of FC.

A one-way, repeated-measures analysis of variance (ANOVA) was used to assess that the SoFC differed statistically significantly across different percentage of top-motion participants added.

3 | RESULTS

3.1 | Pain patients have greater head motion

Compared with healthy participants, CBP participants had statistically significantly greater head motion during scanning ($t_{308} = 9.139$, $p < .001$) (Figure 3a), and the association between motion and pain intensity (numerical rating scale, 0–100; 0 = no pain, 100 = worst pain imaginable) was also statistically significant ($r = .178$, $p = .036$) (Figure 3b); however, neither the effect of sex ($t_{140} = 0.223$, $p = .823$; Figure 2c) nor age ($r = .035$, $p = .680$; Figure 2d) on head motion was statistically significant. In healthy participants, there existed statistically significant difference in head motion between female and male participants ($t_{165} = 3.178$, $p = .002$) (Figure 3e), and age was statistically significantly correlated with motion ($r = .297$, $p < .001$) (Figure 3f).

3.2 | Statistically significant associations between motion and dissimilarity of FC in both healthy and CBP participants

On a group level, the existence of motion effects after preprocessing was still evident, as indicated by the statistically significant inverse association between motion represented by mFD and SoFC. In healthy participants, as shown in Figure 4a,b, this association was observed in all four preprocessing methods (*conventional* [$r = -.541$], *scrub* [$r = -.495$], *ICA-AROMA* [$r = -.504$], and *FIX* [$r = -.517$] with MNI152 as a template and *conventional* [$r = -559$], *scrub* [$r = -.521$], *ICA-AROMA* [$r = -.513$], and *FIX* [$r = -.532$]) with CN200 as a template. The population template effect is minor. When the same data analysis procedure was applied to CBP participants with MNI152 as a template, as shown in Figure 4c, the results were similar (*conventional* [$r = -.563$], *scrub* [$r = -.639$], *ICA-AROMA* [$r = -.595$], and *FIX* [$r = -.607$]). To ensure the relationship between mFD and SoFC was not confounded by age, we performed partial correlations to assess the relationship between mFD and SoFC independent of age. The results were robust, even after adjusting for age ($r = -.489$ [*conventional*], $r = -.436$ [*scrubbing*], $r = -.437$ [*AROMA*], and $r = -.454$ [*FIX*] for healthy participants with MNI152 as a template; $r = -.576$ [*conventional*], $r = -.650$ [*scrubbing*]; $r = -.606$ [*AROMA*], and $r = -.617$ [*FIX*] for CBP participant with MNI152 as a template), which implies that while age is weakly associated with SoFC, it does not share variance with mFD.

3.3 | SoFC derived from *scrub* is more similar to that from *conventional*, than *ICA-AROMA* or *FIX*

SoFC derived from *scrub* is more similar to that from *conventional*, than *ICA-AROMA* or *FIX*. As shown in Figure 5a, for healthy participants, the correlations of SoFC between *scrub* and the three other preprocessing methods (*conventional*, *ICA-AROMA*, and *FIX*) were 0.965, 0.772, and 0.812, respectively. The same trend was observed

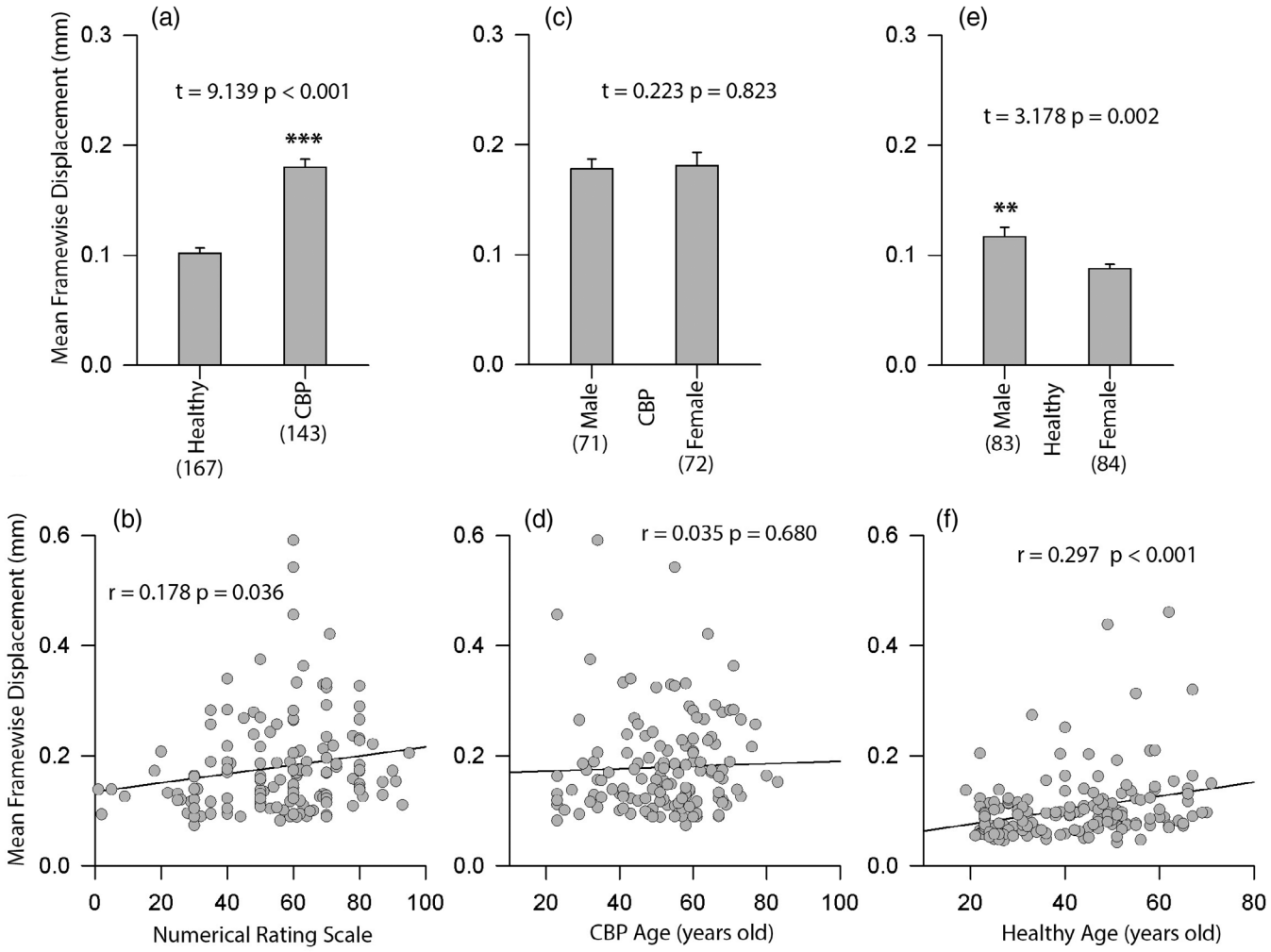

FIGURE 3 Pain patients have greater head motion. (a) Chronic back pain (CBP) patients have greater motion than healthy participants (t_{308} = 9.139, p < .001). For CBP patients, (b) pain intensity (numerical rating scale, 0–100; 0 = no pain, 100 = worst pain imaginable) was statistically significantly correlated with motion (r = .178, p = .036), but (c) there was no statistically significant difference between male and female (t_{140} = 0.223, p = .823), and (d) age was not statistically significantly correlated with motion (r = .035, p = .680). For healthy participants, (e) there was a statistically significant difference between male and female (t_{165} = 3.178, p = .002), and (f) age was statistically significantly correlated with motion (r = .297, p < .001)

in CBP participants (Figure 5b) and the correlations of SoFC between *scrub* and the three other threes (*conventional*, *ICA-AROMA*, and *FIX*) were 0.899, 0.882, and 0.755, respectively. In addition, the correlation of SoFC between *ICA-AROMA* and *FIX*-preprocessing was 0.798 (healthy) and 0.759 (CBP).

3.4 | Participants with the greatest motion determined the strength of the association between motion and dissimilarity of FC

From the group perspective, there existed statistically significant associations between motion and dissimilarity of FC in both healthy and CBP participants. However, the variance of the association was most from greatest-motion participants. For healthy participants (Figure 6a solid curves), when the percentage of greatest-motion participants removed was varied from 0 to 20, the slope of the remaining participants gradually changed from −0.7367 (*conventional*), −0.7279 (*scrub*), −0.5979 (*ICA-AROMA*), and −0.6194 (*FIX*) to −0.1338 (*conventional*), −0.1376 (*scrub*), −0.1663 (*ICA-AROMA*), and −0.0905 (*FIX*). For CBP participants (Figure 6a dotted curves), when the percentage of greatest-motion participants was varied from 0 to 40, the slope of the remaining participants changed from −1.0187 (*conventional*), −1.0472 (*scrub*), −1.1288 (*ICA-AROMA*), and −1.0222 (*FIX*) to −0.1584 (*conventional*), −0.1894 (*scrub*), −0.1047 (*ICA-AROMA*), and −0.1509 (*FIX*). Moreover, the intersections with the line of *mFD threshold* = 0.2 mm (see arrows in Figure 6b) were critical points for both groups, where the corresponding slope curves became flat from steep significantly (see arrows in Figure 6a), indicating the linear relationships between motion and dissimilarity of FC in both healthy and CBP were mostly determined by greatest-motion participants.

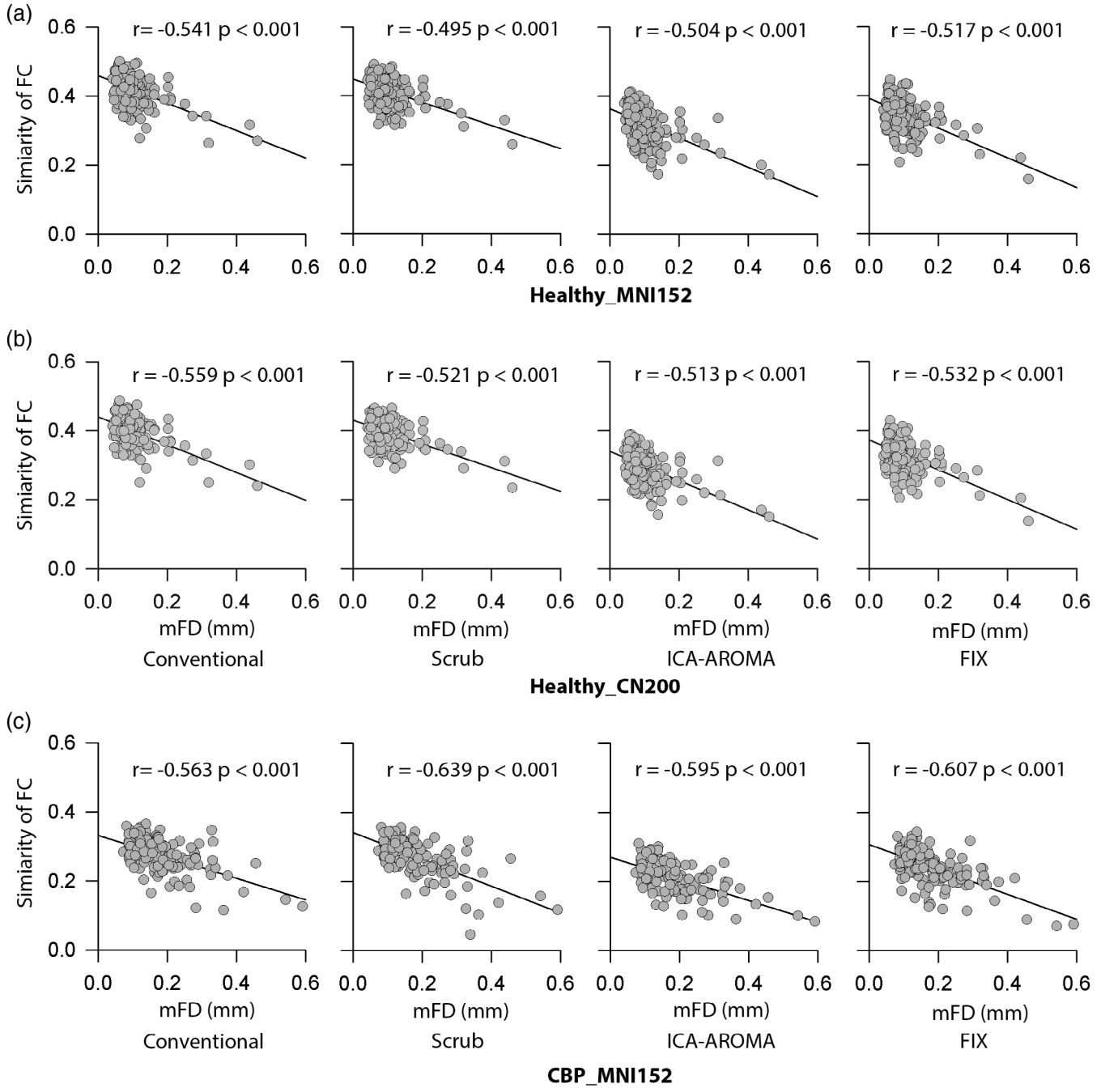

FIGURE 4 Statistically significant inverse association between mean framewise displacement (mFD) and similarity of functional connectivity (SoFC) in both healthy and chronic back pain (CBP) participants. (a) In healthy participants, a statistically significant negative correlation was observed between mFD and SoFC for all four preprocessing methods ($p < .001$) (*conventional* [$r = -.541$], *scrub* [$r = -.495$], *ICA-AROMA* [$r = -.504$], and *FIX* [$r = -.517$]). (b) When using the CN200 template for healthy participants, a statistically significant negative correlation was observed between mFD and SoFC for all four preprocessing methods ($p < .001$) (*conventional* [$r = -.559$], *scrub* [$r = -.521$], *ICA-AROMA* [$r = -.513$], and *FIX* [$r = -.532$]). (c) In CBP participants with MNI152 as the template, a statistically significant negative correlation was observed between mFD and SoFC for all four preprocessing methods ($p < .001$) (*conventional* [$r = -.563$], *scrub* [$r = -.639$], *ICA-AROMA* [$r = -.595$], and *FIX* [$r = -.607$])

3.5 | SoFC was statistically significantly increased following removal of top-motion participants

As shown in Figure 6c (the top four solid lines), when the participants with the greatest motion in healthy group were gradually added from 0 to 20% to randomly ordered lower-motion participants, the results of one-way, repeated-measures ANOVA revealed a statistically significant effect of the percentage on the SoFC. ($F(10,100) = 316.7$, $F(10,100) = 353.3$, $F(10,100) = 832.1$, $F(10,100) = 698.7$, $p < .001$ for *conventional*, *scrub*, *ICA-AROMA*, and *FIX*-preprocessing, respectively).

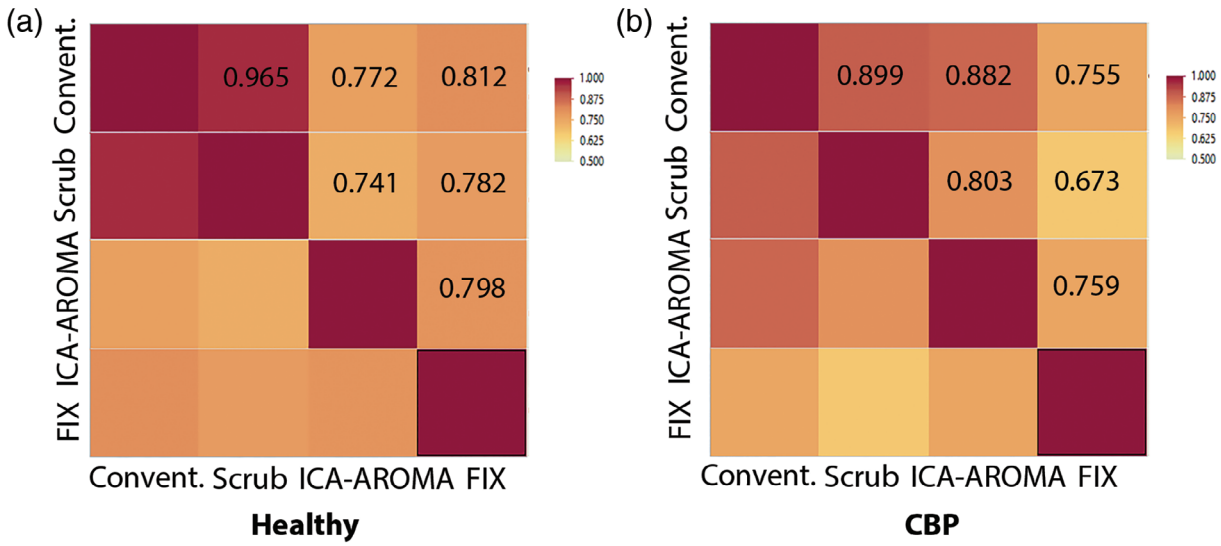

FIGURE 5 Correlation heatmaps of the similarity of functional connectivity derived from conventional, scrub, ICA-AROMA, and FIX-preprocessing methods. (a) In healthy participants, the correlations of similarity of functional connectivity between *scrub* and the three other preprocessing methods (*conventional*, *ICA-AROMA*, and *FIX*) were 0.965, 0.772, and 0.812, respectively. The correlation of similarity of functional connectivity between ICA-AROMA and FIX-preprocessing was 0.798. (b) In CBP participants, the correlations of similarity of functional connectivity between *scrub* and the three other preprocessing methods (*conventional*, *ICA-AROMA*, and *FIX*) were 0.899, 0.882, and 0.755, respectively. The correlation of similarity of functional connectivity between *ICA-AROMA* and *FIX*-preprocessing was 0.759

Bonferroni-corrected post hoc pairwise comparisons revealed that each pairwise difference was statistically significant ($p < .001$), suggesting that the SoFC statistically significantly decreased as a function of the percentage of greater-motion participants added. This phenomenon was observed in CBP group as well (Figure 6c, the bottom four dotted lines). When greater-motion participants were added gradually from 0% to 20% to randomly ordered lower-motion participants, the effects of the percentage on SoFC were again statistically significant ($F(10,84) = 377.1$, $F(10,84) = 802.6$, $F(10,84) = 456.7$, $F(10,84) = 536.1$, $p < .001$ for *conventional*, *scrub*, *ICA-AROMA*, and *FIX*-preprocessing, respectively). Bonferroni-corrected post hoc pairwise comparisons revealed that each pairwise difference was statistically significant ($p < .001$), suggesting that the SoFC significantly decreased as a function of the percentage of greater-motion participants added.

4 | DISCUSSION

Here, we developed and examined a new group-level QC metric to help control for the effects of head motion on FC. We found that (a) pain patients had greater motion and (b) dissimilarity of FC uncovers the influence of participant's motion. Importantly, this relationship is independent of population, scanner, and preprocessing method. Participants with the greatest motion determined the strength of the association between motion and dissimilarity of FC.

Although it is commonly assumed that participants with CBP have elevated motion accompanied with statistically significantly greater confounds than healthy participants, to the best of our knowledge, this study is the first to quantify the effects of head motion and pain intensity. The results shown in Figure 3 indicate that pain or pain-related disorders, like anxiety (de Heer et al., 2014), influence head motion in CBP patients, which was substantial enough that it seems to dwarf the sex and age effects on motion that existed in healthy participants. Considering that motion caused by pain or the pain-related discomfort has a large influence, it is necessary to take preventive strategies; for instance, shortening the duration of scanning sessions, taking a break before fMRI scanning, paying more attention and reminding the patients to remain still during scanning, or even training with a mock MRI to reduce anxiety before scanning (Zaitsev, Maclaren et al. 2015).

The dissimilarity of FC due to motion represents the dissimilarity of each participant's FC relative to the rest in sample, indicating motion-induced BOLD signals increase the distinctiveness of individuals relative to the rest of their sample. At the voxel level, disruption caused by motion decreases the BOLD signal and the magnitude of the signal loss is associated with the extent of motion (Satterthwaite et al., 2013). In addition, more studies indicate that head motion can be a neurobiological trait, contributing to the dissimilarity of FC in the region of default-mode network (Zeng et al., 2014; Zhou et al., 2016). Thus, preprocessing methods for removing motion-related artifacts improve fMRI data quality without necessarily totally correcting the data (Power et al., 2014). At the ROI level, except for those voxels that share disruption produced by motion, the BOLD signal of an ROI extracted as an average over its constituent voxels is diminished because the disruption could extend for tens of seconds and distort hemodynamic response across voxels, even after motion correction (Byrge & Kennedy, 2018; Power et al., 2015), in turn introducing spurious common variance across time points from different regions

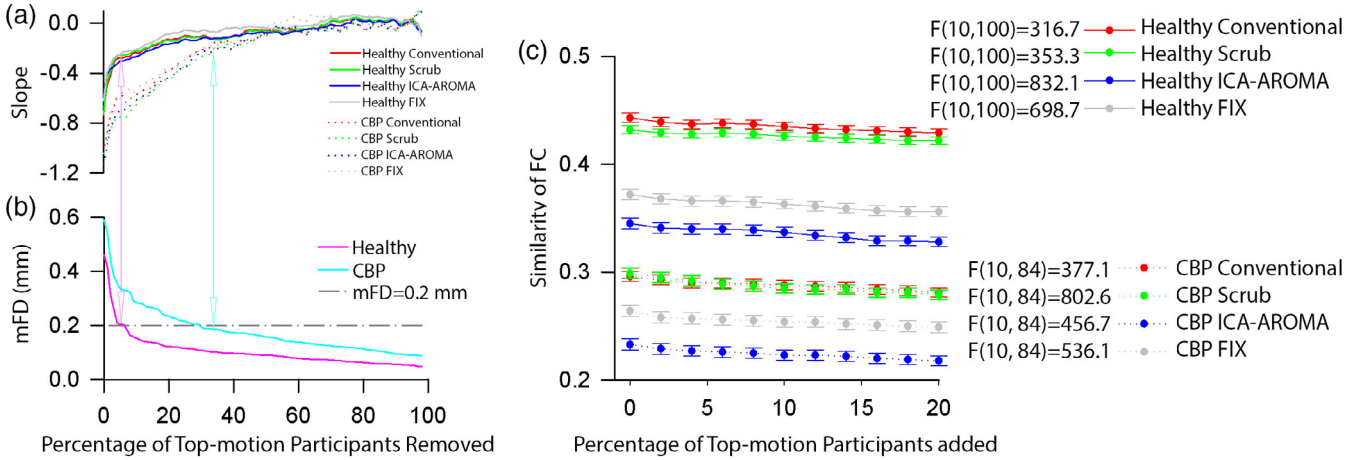

FIGURE 6 Participants with the greatest motion determined the strength of the association between motion and dissimilarity of functional connectivity (a) In healthy participants (solid curves), when the percentage of greatest-motion participants removed was varied from 0 to 20, the slope of the remaining participants gradually changed from −0.7367 (*conventional*), −0.7279 (*scrub*), −0.5979 (*ICA-AROMA*), and −0.6194 (*FIX*) to −0.1338 (*conventional*), −0.1376 (*scrub*), −0.1663 (*ICA-AROMA*), and −0.0905 (*FIX*). In chronic back pain (CBP) participants (dotted curves), when the percentage of greatest-motion participants was varied from 0 to 40, the slope of the remaining participants changed from −1.0187 (*conventional*), −1.0472 (*scrub*), −1.1288 (*ICA-AROMA*), and −1.0222 (*FIX*) to −0.1584 (*conventional*), −0.1894 (*scrub*), −0.1047 (*ICA-AROMA*), and −0.1509 (*FIX*). (b) Depicted the relationship between the percentage of the greatest-motion participants removed and the mFD above which the corresponding participants were removed from the study group and the regression slope between mFD and SoFD in the remaining participants were estimated. CBP had higher mFD than healthy at the same percentage. The intersections with the line of *mFD* = 0.2 mm (arrows) were critical points for both groups, where the corresponding slope curves (see arrows in (a) became flat from steep significantly). (c) In healthy participants (the top four solid lines), when participants with the greatest motion were gradually added from 0 to 20% to randomly ordered bottom-motion participants, the results of one-way, repeated-measures analysis of variance (ANOVA) revealed a statistically significant effect of the percentage on the ($F(10,100) = 316.7$, $F(10,100) = 353.3$, $F(10,100) = 832.1$, $F(10,100) = 698.7$, $p < .001$ for *conventional*, *scrub*, *ICA-AROMA*, and *FIX*-preprocessing, respectively). Bonferroni-corrected post hoc pairwise comparisons revealed that each pairwise difference was statistically significant ($p < .001$), suggesting that the similarity of functional connectivity significantly decreased as a function of the percentage of greatest-motion participants added. Similarly, in CBP participants (the bottom four dotted lines), when greatest-motion participants were added gradually from 0 to 20% to randomly ordered lower-motion participants, the results of one-way, repeated-measures ANOVA revealed a statistically significant effect of the percentage on SoFC ($F(10,84) = 377.1$, $F(10,84) = 802.6$, $F(10,84) = 456.7$, $F(10,84) = 536.1$, $p < .001$ for *conventional*, *scrub*, *ICA-AROMA*, and *FIX*-preprocessing, respectively). Bonferroni-corrected post hoc pairwise comparisons revealed that each pairwise difference was statistically significant ($p < .001$), suggesting that the similarity of functional connectivity significantly decreased as a function of the percentage of top-motion participants added

(Caballero-Gaudes & Reynolds, 2017). As a result, at the participant level, the strength of FC, calculated using Pearson correlation coefficients between ROI BOLD signals, decreases accordingly, except for ROIs that are (a) close and prone to motion, or (b) are distant but with similar motion artifacts (Power et al., 2015). In the end, this disruption due to motion is amplified by dissimilarity of FC at group level, which is evidenced by Figure 3, and independent of participant population, scanner type, or preprocessing method. The observation that dissimilarity of FC reflects the effect of a participant's motion at the group level reemphasizes the impairment of motion to quality of fMRI data even though the data has been preprocessed at participant level. Such findings indicate the necessity of other motion-removal methods, like prospective motion correction (Hoinkiss et al., 2019; Todd, Josephs, Callaghan, Lutti, & Weiskopf, 2015; Zaitsev et al., 2017) or multiecho imaging techniques (Power et al., 2018).

By selecting a suitable percentage of participants with greater motion (e.g., the percentage corresponding to line of mFD = 0.2 mm shown in Figure 6a,b), the slope of the correlation between mFD and dissimilarity of FC in the remaining participants decreases substantially for both groups. This characteristic implies that there may exist multiple sources of motion-related noise after preprocessing. The participants with lower motion (mFD ≤0.2 mm in our data) may contain similar noise structure, increasing the similarity in FC. Concurrently, the confounds present in the participants with high motion are qualitatively different from those in low-motion participants, indicating similarity will always be lower for high-motion participants because high-motion has produced their unique noise signatures, irrespective of what preprocessing method is deployed. Incorporating the results shown in Figure 6c that the SoFC increased as a function of the participants removed, for fMRI studies that contain large-scale images of participants and in which sample size is not a considerable concern, like the UK Biobank (Alfaro-Almagro et al., 2018) or German National Cohort (German National Cohort, 2014), the greatest-motion participants, which account for the greatest effect on FC, can be removed from the group. We suggest that if a group data set is large enough, participants with large motion in the data set be removed to make the regression slope between mean FD and SoFC as flat as possible.

One limitation of our study was the different TRs between groups, which made it difficult to directly compare FD measures. Moreover, the long TR time in the control group precluded assessments of subtle variations in head motion. In the future, we will systematically investigate how preprocessing methods affect SoFC and how distance- and location-distributions of FC vary and interact with SoFC as higher-motion participants are removed.

In conclusion, we found that dissimilarity of FC uncovers the influence of participant's motion, and this relationship is independent of population, scanner, and preprocessing method. Participants with the greatest motion determined the strength of the association between motion and dissimilarity of FC. A new group-based QC strategy is proposed: if a group data set is large enough, participants with large motion in the data set be removed to make the regression slope between mean FD and SoFC as flat as possible.

ACKNOWLEDGMENTS

The authors thank National Institutes of Health (grant 1P50DA044121-01A1) for funding for data analysis. This material is based upon work supported by the National Science Foundation Graduate Research Fellowship under grant No. DGE-1324585.

DATA AVAILABILITY STATEMENT

All data will be available in http://openpain.org after the manuscript is accepted.

ORCID

A. Vania Apkarian https://orcid.org/0000-0002-9788-7458
Lejian Huang https://orcid.org/0000-0003-1753-2372

REFERENCES

Alfaro-Almagro, F., Jenkinson, M., Bangerter, N. K., Andersson, J. L. R., Griffanti, L., Douaud, G., … Smith, S. M. (2018). Image processing and quality control for the first 10,000 brain imaging datasets from UK Biobank. *NeuroImage*, *166*, 400–424. https://doi.org/10.1016/j.neuroimage.2017.10.034

Baliki, M. N., Petre, B., Torbey, S., Herrmann, K. M., Huang, L., Schnitzer, T. J., … Apkarian, A. V. (2012). Corticostriatal functional connectivity predicts transition to chronic back pain. *Nature Neuroscience*, *15*(8), 1117–1119. https://doi.org/10.1038/nn.3153

Byrge, L., & Kennedy, D. P. (2018). Identifying and characterizing systematic temporally-lagged BOLD artifacts. *NeuroImage*, *171*, 376–392. https://doi.org/10.1016/j.neuroimage.2017.12.082

Caballero-Gaudes, C., & Reynolds, R. C. (2017). Methods for cleaning the BOLD fMRI signal. *NeuroImage*, *154*, 128–149. https://doi.org/10.1016/j.neuroimage.2016.12.018

Ciric, R., Rosen, A. F. G., Erus, G., Cieslak, M., Adebimpe, A., Cook, P. A., … Satterthwaite, T. D. (2018). Mitigating head motion artifact in functional connectivity MRI. *Nature Protocols*, *13*(12), 2801–2826. https://doi.org/10.1038/s41596-018-0065-y

de Heer, E. W., Gerrits, M. M., Beekman, A. T., Dekker, J., van Marwijk, H. W., de Waal, M. W., … van der Feltz-Cornelis, C. M. (2014). The association of depression and anxiety with pain: A study from NESDA. *PLoS One*, *9*(10), e106907. https://doi.org/10.1371/journal.pone.0106907

German National Cohort Consotrium. (2014). The German National Cohort: Aims, study design and organization. *European Journal of Epidemiology*, *29*(5), 371–382. https://doi.org/10.1007/s10654-014-9890-7

Hoinkiss, D. C., Erhard, P., Breutigam, N. J., von Samson-Himmelstjerna, F., Gunther, M., & Porter, D. A. (2019). Prospective motion correction in functional MRI using simultaneous multislice imaging and multislice-to-volume image registration. *NeuroImage*, *200*, 159–173. https://doi.org/10.1016/j.neuroimage.2019.06.042

Huang, S., Wakaizumi, K., Wu, B., Shen, B., Wu, B., Fan, L., … Huang, L. (2019). Whole-brain functional network disruption in chronic pain with disk herniation. *Pain*, *160*(12), 2829–2840. https://doi.org/10.1097/j.pain.0000000000001674

Igata, N., Kakeda, S., Watanabe, K., Nozaki, A., Rettmann, D., Narimatsu, H., … Korogi, Y. (2017). Utility of real-time prospective motion correction (PROMO) for segmentation of cerebral cortex on 3D T1-weighted imaging: Voxel-based morphometry analysis for uncooperative patients. *European Radiology*, *27*(8), 3554–3562. https://doi.org/10.1007/s00330-016-4730-7

Jenkinson, M., Bannister, P., Brady, M., & Smith, S. (2002). Improved optimization for the robust and accurate linear registration and motion correction of brain images. *NeuroImage*, *17*(2), 825–841. https://doi.org/10.1006/nimg.2002.1132

Malfliet, A., Coppieters, I., van Wilgen, P., Kregel, J., de Pauw, R., Dolphens, M., & Ickmans, K. (2017). Brain changes associated with cognitive and emotional factors in chronic pain: A systematic review. *European Journal of Pain*, *21*(5), 769–786. https://doi.org/10.1002/ejp.1003

Murphy, K., Birn, R. M., Handwerker, D. A., Jones, T. B., & Bandettini, P. A. (2009). The impact of global signal regression on resting state correlations: Are anti-correlated networks introduced? *NeuroImage*, *44*(3), 893–905. https://doi.org/10.1016/j.neuroimage.2008.09.036

Parkes, L., Fulcher, B., Yucel, M., & Fornito, A. (2018). An evaluation of the efficacy, reliability, and sensitivity of motion correction strategies for resting-state functional MRI. *NeuroImage*, *171*, 415–436. https://doi.org/10.1016/j.neuroimage.2017.12.073

Paulauskas, V. I., & Rachkauskas, A. I. U. (1989). *Approximation theory in the central limit theorems—Exact results in Banach spaces*. Dordrecht, Netherlands: Kluwer Academic Publishers.

Power, J. D., Cohen, A. L., Nelson, S. M., Wig, G. S., Barnes, K. A., Church, J. A., … Petersen, S. E. (2011). Functional network organization of the human brain. *Neuron*, *72*(4), 665–678. https://doi.org/10.1016/j.neuron.2011.09.006

Power, J. D., Mitra, A., Laumann, T. O., Snyder, A. Z., Schlaggar, B. L., & Petersen, S. E. (2014). Methods to detect, characterize, and remove motion artifact in resting state fMRI. *NeuroImage*, *84*, 320–341. https://doi.org/10.1016/j.neuroimage.2013.08.048

Power, J. D., Plitt, M., Gotts, S. J., Kundu, P., Voon, V., Bandettini, P. A., & Martin, A. (2018). Ridding fMRI data of motion-related influences: Removal of signals with distinct spatial and physical bases in multiecho data. *Proceedings of the National Academy of Sciences of the United States of America*, *115*(9), E2105–E2114. https://doi.org/10.1073/pnas.1720985115

Power, J. D., Schlaggar, B. L., & Petersen, S. E. (2015). Recent progress and outstanding issues in motion correction in resting state fMRI. *NeuroImage*, *105*, 536–551. https://doi.org/10.1016/j.neuroimage.2014.10.044

Pruim, R. H., Mennes, M., van Rooij, D., Llera, A., Buitelaar, J. K., & Beckmann, C. F. (2015). ICA-AROMA: A robust ICA-based strategy for removing motion artifacts from fMRI data. *NeuroImage*, *112*, 267–277. https://doi.org/10.1016/j.neuroimage.2015.02.064

Salimi-Khorshidi, G., Douaud, G., Beckmann, C. F., Glasser, M. F., Griffanti, L., & Smith, S. M. (2014). Automatic denoising of functional MRI data: Combining independent component analysis and

hierarchical fusion of classifiers. *NeuroImage*, *90*, 449–468. https://doi.org/10.1016/j.neuroimage.2013.11.046

Satterthwaite, T. D., Elliott, M. A., Gerraty, R. T., Ruparel, K., Loughead, J., Calkins, M. E., … Wolf, D. H. (2013). An improved framework for confound regression and filtering for control of motion artifact in the preprocessing of resting-state functional connectivity data. *NeuroImage*, *64*, 240–256. https://doi.org/10.1016/j.neuroimage.2012.08.052

Satterthwaite, T. D., Wolf, D. H., Loughead, J., Ruparel, K., Elliott, M. A., Hakonarson, H., … Gur, R. E. (2012). Impact of in-scanner head motion on multiple measures of functional connectivity: Relevance for studies of neurodevelopment in youth. *NeuroImage*, *60*(1), 623–632. https://doi.org/10.1016/j.neuroimage.2011.12.063

Sladky, R., Friston, K. J., Trostl, J., Cunnington, R., Moser, E., & Windischberger, C. (2011). Slice-timing effects and their correction in functional MRI. *NeuroImage*, *58*(2), 588–594. https://doi.org/10.1016/j.neuroimage.2011.06.078

Smith, A. M., Lewis, B. K., Ruttimann, U. E., Ye, F. Q., Sinnwell, T. M., Yang, Y., … Frank, J. A. (1999). Investigation of low frequency drift in fMRI signal. *NeuroImage*, *9*(5), 526–533. https://doi.org/10.1006/nimg.1999.0435

Smith, S. M., & Brady, J. M. (1997). SUSAN—A new approach to low level image processing. *International Journal of Computer Vision*, *23*(1), 45–78. https://doi.org/10.1023/A:1007963824710

Todd, N., Josephs, O., Callaghan, M. F., Lutti, A., & Weiskopf, N. (2015). Prospective motion correction of 3D echo-planar imaging data for functional MRI using optical tracking. *NeuroImage*, *113*, 1–12. https://doi.org/10.1016/j.neuroimage.2015.03.013

Yang, G., Zhou, S., Bozek, J., Dong, H. M., Han, M., Zuo, X. N., … Gao, J. H. (2020). Sample sizes and population differences in brain template construction. *NeuroImage*, *206*, 116318. https://doi.org/10.1016/j.neuroimage.2019.116318

Yuan, W., Altaye, M., Ret, J., Schmithorst, V., Byars, A. W., Plante, E., & Holland, S. K. (2009). Quantification of head motion in children during various fMRI language tasks. *Human Brain Mapping*, *30*(5), 1481–1489. https://doi.org/10.1002/hbm.20616

Zaitsev, M., Akin, B., LeVan, P., & Knowles, B. R. (2017). Prospective motion correction in functional MRI. *NeuroImage*, *154*, 33–42. https://doi.org/10.1016/j.neuroimage.2016.11.014

Zaitsev, M., Maclaren, J., & Herbst, M. (2015). Motion artifacts in MRI: A complex problem with many partial solutions. *Journal of Magnetic Resonance Imaging*, *42*(4), 887–901. https://doi.org/10.1002/jmri.24850.

Zeng, L. L., Wang, D., Fox, M. D., Sabuncu, M., Hu, D., Ge, M., … Liu, H. (2014). Neurobiological basis of head motion in brain imaging. *Proceedings of the National Academy of Sciences of the United States of America*, *111*(16), 6058–6062. https://doi.org/10.1073/pnas.1317424111

Zhou, Y., Chen, J., Luo, Y. L. L., Zheng, D., Rao, L.-L., Li, X., … Zuo, X.-N. (2016). Genetic overlap between in-scanner head motion and the default network connectivity. *bioRxiv*, *11*, 087023. https://doi.org/10.1101/087023

How to cite this article: Yang L, Wu B, Fan L, et al. Dissimilarity of functional connectivity uncovers the influence of participant's motion in functional magnetic resonance imaging studies. *Hum Brain Mapp*. 2020;1–11. https://doi.org/10.1002/hbm.25255